

# Suppression of NLRP3 inflammasome by $\gamma$ -tocotrienol ameliorates type 2 diabetes<sup>S</sup>

Yongeun Kim,<sup>1</sup> Wei Wang,<sup>1</sup> Meshail Okla, Inhae Kang, Regis Moreau, and Soonkyu Chung<sup>2</sup>

Department of Nutrition and Health Sciences, University of Nebraska-Lincoln, Lincoln, NE 68583

**Abstract** The Nod-like receptor 3 (NLRP3) inflammasome is an intracellular sensor that sets off the innate immune system in response to microbial-derived and endogenous metabolic danger signals. We previously reported that  $\gamma$ -tocotrienol ( $\gamma$ T3) attenuated adipose tissue inflammation and insulin resistance in diet-induced obesity, but the underlying mechanism remained elusive. Here, we investigated the effects of  $\gamma$ T3 on NLRP3 inflammasome activation and attendant consequences on type 2 diabetes.  $\gamma$ T3 repressed inflammasome activation, caspase-1 cleavage, and interleukin (IL) 1 $\beta$  secretion in murine macrophages, implicating the inhibition of NLRP3 inflammasome in the anti-inflammatory and antipyroptotic properties of  $\gamma$ T3. Furthermore, supplementation of leptin-receptor KO mice with  $\gamma$ T3 attenuated immune cell infiltration into adipose tissue, decreased circulating IL-18 levels, preserved pancreatic  $\beta$ -cells, and improved insulin sensitivity. Mechanistically,  $\gamma$ T3 regulated the NLRP3 inflammasome via a two-pronged mechanism: 1) the induction of A20/TNF- $\alpha$  interacting protein 3 leading to the inhibition of the TNF receptor-associated factor 6/nuclear factor  $\kappa$ B pathway and 2) the activation of AMP-activated protein kinase/autophagy axis leading to the attenuation of caspase-1 cleavage. Collectively, we demonstrated, for the first time, that  $\gamma$ T3 inhibits the NLRP3 inflammasome thereby delaying the progression of type 2 diabetes. This study also provides an insight into the novel therapeutic values of  $\gamma$ T3 for treating NLRP3 inflammasome-associated chronic diseases.—Kim, Y., W. Wang, M. Okla, I. Kang, R. Moreau, and S. Chung. **Suppression of NLRP3 inflammasome by  $\gamma$ -tocotrienol ameliorates type 2 diabetes.** *J. Lipid Res.* 2016. 57: 66–76.

**Supplementary key words** inflammation • obesity • vitamin E • insulin signaling • diet and dietary lipids • NOD-like receptor protein 3 • A20 • caspase 1

$\gamma$ -Tocotrienol ( $\gamma$ T3) is an isomer of unsaturated vitamin E known to exert potent anti-inflammatory functions in various cell types including macrophages, adipocytes, and several cancerous cells (1). There is emerging evidence suggesting that  $\gamma$ T3 promotes insulin sensitivity, attenuates

adipose inflammation, and decreases hepatosteatosis (2–5). The inhibition of nuclear factor  $\kappa$ B (NF $\kappa$ B) signaling has been implicated in the underlying mechanism by which  $\gamma$ T3 regulates cellular processes from cell proliferation to insulin sensitization (5–7). However, the fundamental molecular mechanism whereby  $\gamma$ T3 modulates inflammation in diverse cell types and mitigates the accompanying pathophysiological sequelae is unknown.

Inflammasomes are multiprotein cytosolic receptors that detect damage signals triggered by invasion of pathogens or by metabolic stresses leading to production of type 1 interferons and proinflammatory cytokines. Excessive activation of inflammasomes is frequently associated with the prevalence of various chronic inflammatory diseases including multiple sclerosis, Alzheimer's disease, atherosclerosis, age-related macular degeneration, and type 1 and 2 diabetes (8). Notably, a critical role of the NOD-like receptor protein 3 (NLRP3) inflammasome has been established in the progression of insulin resistance to type 2 diabetes (9–11). The assembly of inflammasomes is initiated by scaffolding proteins, either NLR (NOD-like receptor proteins) or AIM2 (absent in melanoma 2). It subsequently recruits adaptor protein ASC (apoptosis-associated speck-like protein containing a caspase recruitment domain) and pro-caspase-1. Upon assembly of the inflammasome, caspase-1 becomes active and in turn activates proinflammatory cytokines pro-interleukin (IL)-1 $\beta$  and pro-IL-18 through proteolytic cleavage, resulting in the secretion of IL-1 $\beta$  and IL-18 and cell pyroptosis (reviewed in Ref. 12). Activation of the NLRP3 inflammasome

Abbreviations: AMPK, AMP-activated protein kinase; BMDM, bone marrow-derived macrophage; BW, body weight; CM, conditioned medium; CQ, chloroquine; DAMP, damage-associated molecular pattern;  $\gamma$ T3,  $\gamma$ -tocotrienol; GLuc, *Gaussia* luciferase; GTT, glucose tolerance test; H&E, hematoxylin and eosin; iGLuc, pro-interleukin-1 $\beta$ -*Gaussia* luciferase; iJ774, J774 macrophage stably expressing iGLuc; IL, interleukin; ITT, insulin tolerance test; NF $\kappa$ B, nuclear factor  $\kappa$ B; Ng, nigericin; NLRP3, NOD-like receptor protein 3; PA, palmitate; PAMP, pathogen-associated molecular pattern; qPCR, quantitative PCR; SV, stromal vascular; TNFAIP3, TNF- $\alpha$  interacting protein 3 (same as A20); TRAF6, TNF receptor-associated factor 6; WAT, white adipose tissue.

<sup>1</sup>Y. Kim and W. Wang contributed equally to this work.

<sup>2</sup>To whom correspondence should be addressed.

e-mail: chung4@unl.edu

<sup>S</sup>The online version of this article (available at <http://www.jlr.org>) contains a supplement.

This work was supported by an American Heart Association Scientist Development Grant (National) 13SDG14410043 (S.C.).

Manuscript received 18 August 2015 and in revised form 14 November 2015.

Published, JLR Papers in Press, December 1, 2015

DOI 10.1194/jlr.M062828

is regulated by two discrete signaling cues: the priming and assembly of the inflammasome. The priming of NLRP3 inflammasome consists of the transcription of inflammasome components and requires NF $\kappa$ B-mediated transcription of *pro-IL-1 $\beta$* , *pro-IL-18*, and *Nlrp3* (13). Subsequently, the inflammasome assembles in response to the engagement of pattern recognition receptors by pathogen-associated molecular pattern (PAMP) or damage-associated molecular pattern (DAMP) endogenous signals (sterile inflammation); the latter include FFA, free cholesterol, uric acid, and ATP. One of the key mechanisms by which inflammasome assembly can be repressed is autophagic degradation of these deleterious molecular factors (reviewed in Ref. 14).

Our previous work as well as others has shown that  $\gamma$ T3 can block NF $\kappa$ B activation (5–7) and stimulate AMP-activated protein kinase (AMPK) and autophagy in a variety of cell types (15–18). In the present study, we ask whether  $\gamma$ T3 represses the NLRP3 inflammasome and associated inflammatory processes in type 2 diabetes by modulating NF $\kappa$ B, AMPK, and autophagy signaling pathways. Using murine macrophages and leptin receptor knockout (*db/db*) mice, we clearly show that  $\gamma$ T3 blocks NLRP3 inflammasome activation and ameliorates type 2 diabetes.

## RESEARCH DESIGN AND METHODS

### Chemicals and reagents

$\gamma$ T3 (with 90% purity) was kindly provided by Carotech.  $\gamma$ T3 was prepared as previously described (18). Compound C was purchased from Calbiochem. All other chemicals and reagents were purchased from Sigma Chemical Co., unless otherwise stated.

### Animals

All animal experimental procedures were approved by the Institutional Animal Care and Use Committee at the University of Nebraska-Lincoln. Male BKS.Cg-*Dock7*<sup>tm1.1</sup>*Lep*<sup>db</sup>/J mice (referred to as *db/db* mice) were obtained from Jackson Laboratory. Animals were housed in a specific pathogen-free facility and given free access to food and water. Mice (6 weeks old) were fed a standard AIN93G diet (control) or the AIN93G containing 0.1% (w/w)  $\gamma$ T3 for 8 weeks. Mice were given fresh rations daily. Food and water consumption were measured every day for 3 days during the last week of feeding before euthanasia. Individual body weights were measured weekly.

### Preparation of bone marrow-derived macrophages and stimulation for inflammasome

Primary bone marrow cells were isolated from the femurs of 6- to 10-week-old C57BL/6 mice and stimulated to differentiate for 7–10 days in L-cell conditioned medium (CM) as we described previously (5). The resulting differentiated bone marrow-derived macrophages (BMDMs) were pretreated with  $\gamma$ T3 or vehicle (DMSO) for 24 h, then primed with lipopolysaccharide (LPS) (100 ng/ml) for 1 h, and stimulated either with nigericin (Ng; 6.5  $\mu$ M, a K<sup>+</sup>/H<sup>+</sup> ionophore) for 1 h or palmitate (PA; 400  $\mu$ M complexed with BSA) for 12 h.

### Pro-IL-1 $\beta$ -*Gaussia* luciferase reporter assay

The J774 macrophages stably expressing pro-IL-1 $\beta$ -*Gaussia* luciferase (iGLuc) fusion construct (Fig. 1A) were a generous gift

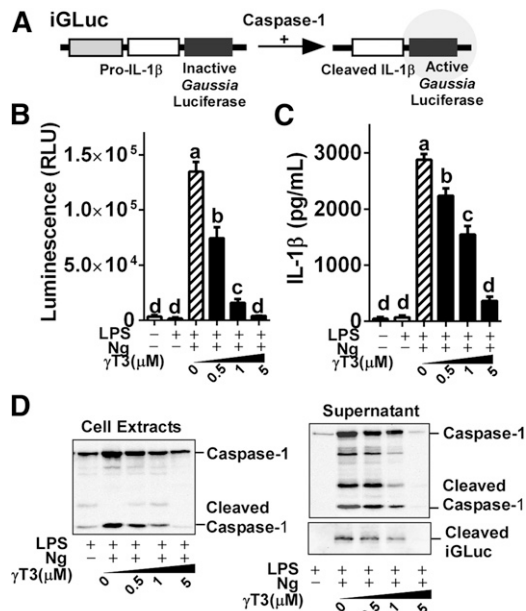


**Fig. 1.**  $\gamma$ T3 suppressed NLRP3 inflammasome procaspase reporter activity in iJ774 macrophages. iJ774 macrophages were preincubated with  $\gamma$ T3 (0–5  $\mu$ M) for 24 h before LPS priming (100 ng/ml for 1 h) and subsequent Ng stimulation. A: Structure of the iGLuc (NLRP3 inflammasome and caspase activity reporter constructs). B: Relative GLuc activity was quantified by luminometer. C: IL-1 $\beta$  secretion (in medium) quantified by ELISA. Results in B and C are shown as the mean  $\pm$  SEM (n = 6). Values not sharing a common letter differ significantly ( $P < 0.05$ ) by one-way ANOVA. D: Cleavage of caspase-1 in cell extract and supernatant. Results in D are representative of triplicate samples.

from Dr. Hornung (hereafter referred to as iJ774 macrophages) (19). iJ774 macrophages were cultured in DMEM supplemented with L-glutamine, sodium pyruvate, and 10% (v/v) FBS (Gibco). To determine *Gaussia* luciferase (GLuc) activity, the BioLux GLuc assay kit (NEB Inc.) was used and read with a Synergy H1 multimode reader (BioTek). The cleavage product of the pro-IL-1 $\beta$ -iGLuc fusion protein was detected in the media by Western blot analysis using anti-GLuc antibody (NEB Inc.).

### Glucose and insulin tolerance tests

A glucose tolerance test (GTT) was performed on fasted (overnight) *db/db* mice by intraperitoneal injection of 10% D-glucose solution [0.5 g/kg body weight (BW)]. Blood glucose levels (mg/dl) were measured at 0, 15, 30, 60, and 120 min after injection using a glucometer (Bayer, Contour). Plasma insulin levels at basal and 30 min after glucose intraperitoneal injection were determined by ELISA (Crystal Chem). For insulin tolerance test (ITT), fasted (4 h) *db/db* mice were administered 1 U/kg BW of insulin (Novolin R); blood glucose levels were measured at 0, 15, 30, and 60 min after injection.

### Quantitative real-time PCR

Gene expression analysis was performed as described previously (18). Relative gene expression was determined based on the  $2^{-\Delta\Delta CT}$  method with normalization of the raw data to either *36b4* or *Gapdh* (see primer sequences in supplementary Table 1). For PCR microarray analysis, RT<sup>2</sup> profiler PCR array for mouse inflammasome (PAMM-097ZD) was used according to the manufacturer's instruction (Qiagen). For each treatment, equal amounts of total mRNA obtained from four mice were pooled. The results were analyzed using software provided by Qiagen.

## Immunoblotting, immunoprecipitation, and ELISA

Total cell and tissue extract preparation and Western blot procedures were conducted as we described previously (5). The antibodies recognizing phospho(p)-p38(Thr180/182), TNF- $\alpha$  interacting protein 3 (A20/TNFAIP3), ATG5, p-IKK $\alpha$ / $\beta$  (Ser176/180), K63-linkage polyubiquitin, K48-linkage polyubiquitin, p-p44/42-ERK1/2 (Thr202/204), total (t)-ERK, p-AMPK $\alpha$  (Thr 172), t-AMPK,  $\beta$ -actin, LC3, p62, Beclin-1, I $\kappa$ B $\alpha$ , and p-I $\kappa$ B $\alpha$  (Ser32/36) were purchased from Cell Signaling Technology. Antibodies against NLRP3, TNF receptor-associated factor 6 (TRAF6), and caspase-1 (p20) were purchased from R&D Systems, Santa Cruz Biotechnology, and AdipoGen, respectively. For the immunoprecipitation of ubiquitinated-TRAF6, protein A/G magnetic beads (Pierce) were used according to the manufacturer's instruction. Plasma levels of adiponectin, IL-18, and IL-1 $\beta$  were quantified by using commercial ELISA kits from R&D Systems.

## Isolation of stromal vascular cells and flow cytometric analysis

Epididymal fat pads were collected at the time of necropsy and used for stromal vascular (SV) cell isolation by following the protocol of Orr et al. (20). For cell surface staining, cells were stained for 30 min at room temperature in FCS-PBS buffer (1%) with the following antibodies: FITC-CD4, PE-CD8, and APC/Cy7 CD45 and relative isotypes (BioLegend). SV cells were gated using forward and side scatter characteristics for lymphocytes on the basis of at least 10,000 events using a FACSCalibur<sup>TM</sup> flow cytometer (BD Biosciences). Data were analyzed using FlowJo software (Treestar).

## Hematoxylin and eosin staining, islet size determination, and insulin staining

Paraffin-embedded epididymal adipose tissues from mice were sectioned (10  $\mu$ m) for hematoxylin and eosin (H&E) staining. Paraffin-embedded pancreases were serially sectioned (5  $\mu$ m) at 50  $\mu$ m intervals and used for H&E staining and insulin immunostaining. For determination of average islet size, ~150–200 islets were counted per mouse pancreas from the six serial sections of H and E-stained paraffin block (using Image J software). For insulin staining, pancreas sections were incubated with a primary insulin antibody (dilution 1:50, Dako), followed by incubation with EnVision-AP<sup>TM</sup> (Dako) and visualized using a SIGMA-FAST<sup>TM</sup> Fast Red system with hematoxylin counterstaining.

## siRNA transfection

siRNAs (On-Target smart pool) targeting mouse A20 (*Tnfrsf25*) or nontargeting siRNA control were transfected into iJ774 macrophages at a final concentration of 100 nM using DharmaFECT4 transfection reagent (GE Dharmacon). Forty-eight hours after transfection, cells were washed and stimulated as indicated in the figure legends.

## Statistics

The two-tailed Student's *t*-test was used for statistical analyses of two-group comparisons. Multigroup comparisons were performed by a one-way ANOVA followed by Tukey's multiple comparison test. All statistical analyses were performed using GraphPad Prism 6 (version 6.02).

## RESULTS

### $\gamma$ T3 Inhibited NLRP3 inflammasome activation in macrophages

To test whether  $\gamma$ T3 suppresses NLRP3-inflammasome activation, we first performed the iGLuc reporter assay for

inflammasome and protease activity (Fig. 1A) in iJ774 macrophages. The  $\gamma$ T3 (0–5  $\mu$ M) dose-dependently decreased *Gaussia* luminescence upon Ng stimulation of LPS-primed iJ774 macrophages (Fig. 1B). Similarly, IL-1 $\beta$  secretion in the medium decreased gradually with increasing dose of  $\gamma$ T3 (Fig. 1C). In addition, we observed a stepwise decrease of cleaved caspase-1, a surrogate marker for caspase-1 activation, in both cell extracts and supernatants upon treatment with graded dose of  $\gamma$ T3 (Fig. 1D). We confirmed these results in primary BMDMs where pretreatment with 1  $\mu$ M  $\gamma$ T3 repressed the secretion of IL-1 $\beta$  and IL-18 in LPS-primed Ng-stimulated cells (Fig. 2A). The mRNA levels of *Il-1 $\beta$* , *Il-18*, and *Nlrp3* were also markedly decreased by  $\gamma$ T3 (Fig. 2B), suggesting that  $\gamma$ T3 suppresses the priming of NLRP3 inflammasome. Additionally, the abundance of NLRP3 protein and caspase-1 cleavage were decreased, whereas LC3II and p-AMPK $\alpha$  (Thr172) were increased by  $\gamma$ T3 (Fig. 2C). To determine whether  $\gamma$ T3 is able to suppress DAMP-triggered inflammasome activation, LPS-primed BMDMs were stimulated with 400  $\mu$ M of PA.  $\gamma$ T3 pretreatment (1  $\mu$ M) remarkably reduced: 1) the secretion of IL-1 $\beta$  and IL-18 in the medium (Fig. 2D); 2) the mRNA levels of *Il-1 $\beta$* , *Il-18*, and *Nlrp3* (Fig. 2E); and 3) the protein abundance of NLRP3 and cleaved caspase-1 (Fig. 2F).  $\gamma$ T3 concomitantly induced LC3II accumulation and AMPK phosphorylation (Fig. 2F) implying that the AMP kinase/autophagy axis was stimulated.

### $\gamma$ T3 ameliorated the progression of type 2 diabetes in *db/db* mice

To determine the effectiveness of  $\gamma$ T3 supplementation in preventing the progression of type 2 diabetes, *db/db* mice were fed either an AIN93G diet devoid of  $\gamma$ T3 (control) or an AIN93 diet containing 0.1%  $\gamma$ T3 (1 g/kg diet) for 8 weeks. Feeding  $\gamma$ T3 to *db/db* mice was associated with the improvement of diabetic hyperphagia (Fig. 3A) and diabetic thirst (polydipsia) (Fig. 3B), and a slight but significant increase in body weight (Fig. 3C). Importantly, results show a significant decrease in fasting glucose levels (Fig. 3D), but an increase of adiponectin levels (Fig. 3E).  $\gamma$ T3 also improved glucose disposal during the GTT (Fig. 3F). There was no significant change in fasting insulin levels between the two groups. However, 30 min within the GTT, plasma insulin failed to rise in control mice, whereas in  $\gamma$ T3-fed mice plasma insulin levels were increased ~2-fold (Fig. 3G). During the ITT, the insulin injection (1 U/kg BW) markedly improved glucose clearance to the same extent in both groups of mice (Fig. 3H). H&E staining of pancreatic islet cells revealed that the average islet size was significantly larger in  $\gamma$ T3-fed mice than in controls (Fig. 3I), and the islet size distribution shifted toward larger sizes in  $\gamma$ T3-fed mice (Fig. 3J). Moreover, the percentage of insulin-positive area per islet was significantly higher in  $\gamma$ T3-fed mice than controls (5.9% vs. 2.4%; Fig. 3K). The immunostaining of the islets also showed that islet integrity was better preserved in  $\gamma$ T3-fed mice with a low degree of immune cell infiltration (Fig. 3L). Collectively, these data indicate that  $\gamma$ T3 attenuates the loss of pancreatic  $\beta$ -cells and delays the progression of type 2 diabetes in *db/db* mice.



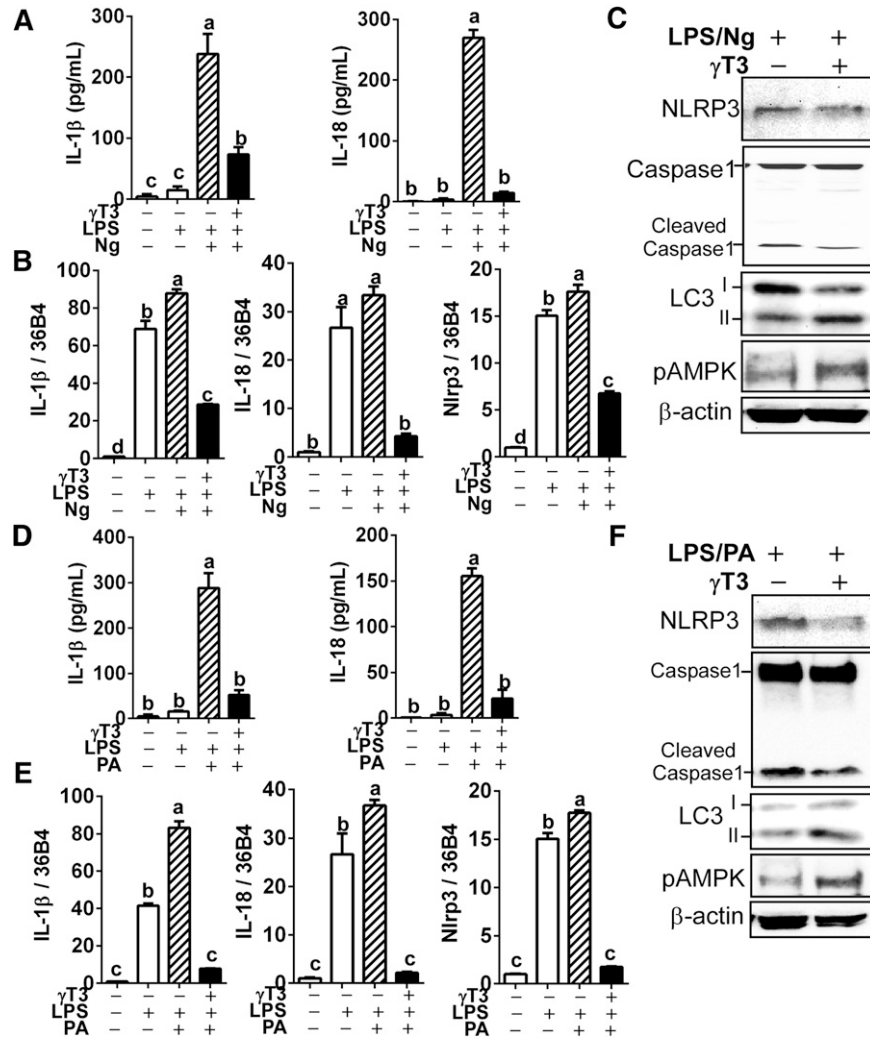


**Fig. 2.**  $\gamma$ T3 inhibited NLRP3 inflammasome in BMDMs. BMDMs were preincubated with vehicle (DMSO) or  $\gamma$ T3 (1  $\mu$ M). Inflammasome activation was triggered by either Ng (A–C) or PA (D, E) in LPS-primed BMDMs. IL-1 $\beta$  and IL-18 secreted in culture medium was measured by ELISA (A, D). The mRNA levels of *Il-1 $\beta$* , *Il-18*, and *Nlrp3* were analyzed by quantitative PCR (qPCR) (B, E). The protein levels of NLRP3, caspase-1, LC3, p-AMPK $\alpha$  (Thr172), and  $\beta$ -actin in cell lysates determined by Western blot (C, F). All data are shown as mean  $\pm$  SEM in A, B, D, and E (n = 6 per group). Values not sharing a common letter differ significantly ( $P < 0.05$ ) by one-way ANOVA. Results in C and F are representative of triplicate samples.

### $\gamma$ T3 suppressed NLRP3 inflammasome activation in peritoneal macrophages of *db/db* mice

We asked whether the observed improvement of type 2 diabetes sequelae by  $\gamma$ T3 was due to the suppression of NLRP3 inflammasome activation and associated inflammatory processes. We found that plasma IL-18 was decreased by  $\sim$ 2-fold in  $\gamma$ T3-fed versus control mice (Fig. 4A), whereas IL-1 $\beta$  levels were below detection limit in both groups. Next, we isolated the peritoneal macrophages from *db/db* mice fed the experimental diets for 8 weeks to carry out further analysis. Consistent with the results in Fig. 1, the mRNA levels of NF $\kappa$ B target genes, which included *Il-6*, *Tnfa*, *Il-1 $\beta$* , *Il-18*, and *Nlrp3*, were significantly downregulated in the macrophages of  $\gamma$ T3-fed mice (Fig. 4B). There was a  $\sim$ 40-fold increase in A20 transcript levels, a negative feedback regulator of NF $\kappa$ B (Fig. 4B). The inflammasome 84-gene array revealed that no gene was

significantly upregulated by  $\gamma$ T3 supplementation. However, six genes (i.e., *Il-12b*, *Nlrp3*, *Nfkbib*, *Nlr5*, *Nlrp4b*, and *Nlrp12*) were differentially downregulated  $>2$ -fold in the macrophages of  $\gamma$ T3-fed mice (Fig. 4C; also see supplementary Table 2). Western blot analyses showed that the macrophages of  $\gamma$ T3-fed mice had less phosphorylated MAP kinase (p-ERK and p38), more I $\kappa$ B $\alpha$  and A20/TNFAIP3, and less NLRP3 and cleaved caspase-1 (Fig. 4D).

We also investigated the role of  $\gamma$ T3 in autophagy in peritoneal macrophages of *db/db* mice. p-AMPK $\alpha$  (Thr 172) as well as markers of autophagic activation, including Beclin-1, autophagy protein 5 (ATG5), and LC3II, were markedly increased by  $\gamma$ T3, whereas p62 was decreased by  $\gamma$ T3 (Fig. 4E). Because p62 is degraded in autolysosome, p62 levels are inversely correlated with autophagic flux. To confirm that the autophagic flux was stimulated by  $\gamma$ T3, BMDMs were treated with chloroquine (CQ), a lysosomal

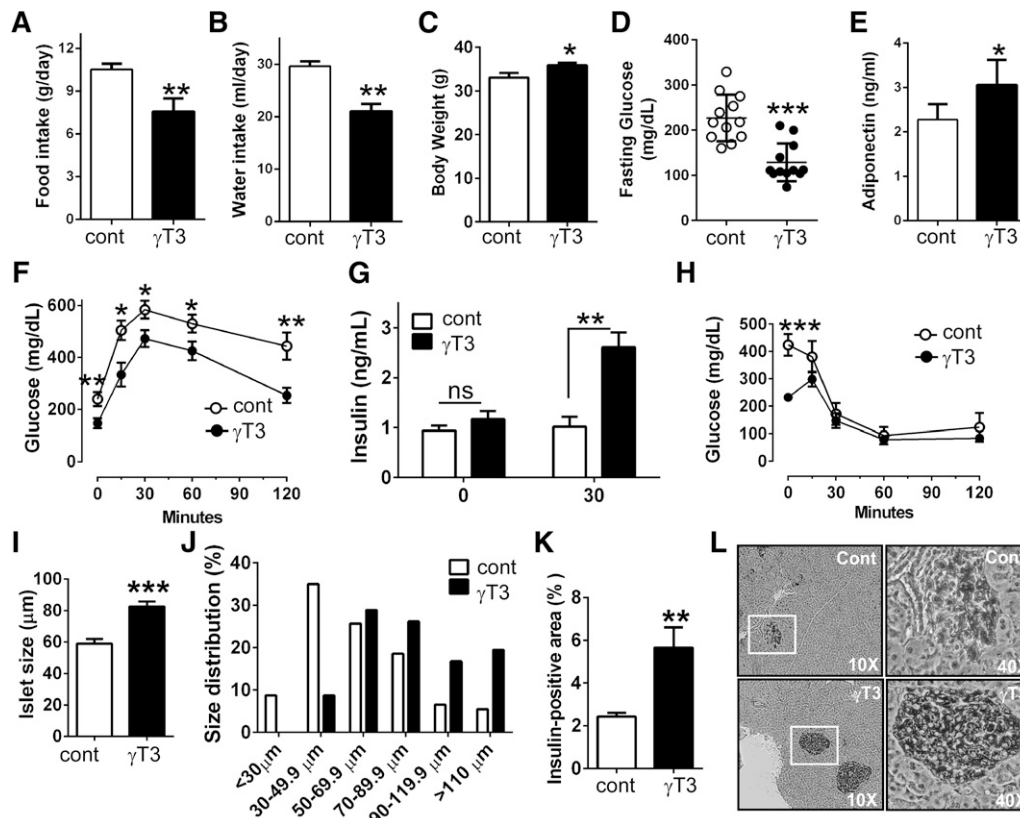


**Fig. 3.**  $\gamma$ T3 ameliorated the progression of type 2 diabetes in *db/db* mice. Male *db/db* mice were fed with either an AIN93G control diet devoid of  $\gamma$ T3 or an AIN93G diet containing 0.1%  $\gamma$ T3 for 8 weeks ( $n = 12$  mice per group). A: Food intake. B: Water intake. C: Body weight. D: Fasting glucose levels. E: Adiponectin levels (ELISA). F: GTT. G: Plasma insulin levels at 0 and 30 min after intraperitoneal glucose injection were quantified by ELISA. H: ITT. I: Average size of islets of Langerhans. J: Relative size distribution of the pancreatic islets. K: Percentage of insulin-positive area/pancreas area. L: Representative images of insulin-positive islet area after immunohistochemical staining of insulin ( $n = 5$ ). All data are shown as mean  $\pm$  SEM. \*  $P < 0.05$ ; \*\*  $P < 0.01$ ; \*\*\*  $P < 0.001$  by Student's *t*-test.

degradation inhibitor.  $\gamma$ T3 (but not control) led to LC3II accumulation and p62 degradation in CQ-treated BMDMs (Fig. 4F) implying that  $\gamma$ T3 coregulates autophagosome formation and inflammasome activation. Taken together, these data revealed that  $\gamma$ T3 decreased NLRP3 inflammasome activation in macrophages of *db/db* mice.

#### $\gamma$ T3 decreased immune cell infiltration into white adipose tissue and preserved insulin sensitivity

The impact of  $\gamma$ T3-mediated suppression of NLRP3 inflammasome activation on adipose tissue inflammation was further investigated in epididymal white adipose tissue (WAT) of *db/db* mice. H&E staining revealed that  $\gamma$ T3 supplementation significantly reduced immune cell infiltration into WAT (Fig. 5A). Flow cytometric analysis of the SV fractions showed that total macrophage infiltration ( $F4/80^+$ ) was decreased by  $\sim 30\%$  in  $\gamma$ T3-fed versus control mice (12.3% vs. 8.3%; Fig. 5B). In addition, *Cd11c* gene expression was substantially decreased in the WAT of  $\gamma$ T3-fed mice (Fig. 5C). In accordance with the anti-inflammatory role of  $\gamma$ T3 in peritoneal macrophages (Fig. 4C), feeding  $\gamma$ T3 to *db/db* mice decreased the mRNA levels of *Il-1 $\beta$* , *Il-18*, and *Nlrp3* but raised those of

*A20* in WAT (Fig. 5D). Flow cytometry data revealed that the total leukocytes ( $CD45^+$ ) and cytotoxic T-cell populations ( $CD45^+/CD8^+$ ) were significantly decreased in the WAT of  $\gamma$ T3-fed mice compared with control WAT (Fig. 5E).

Next, we examined whether  $\gamma$ T3 modulates NLRP3 inflammasome activation in WAT. Our results showed that  $\gamma$ T3 supplementation decreased NLRP3 expression, ERK phosphorylation, and caspase-1 cleavage, but increased protein levels of  $I\kappa B\alpha$  and A20 in epididymal WAT (Fig. 5F). Furthermore, the WAT of  $\gamma$ T3-fed mice exhibited higher AMPK phosphorylation (Thr172) and Beclin-1 and LC3II abundance, but lower abundance of p62 compared with control mice (Fig. 5G), collectively suggesting activation of the AMPK/autophagy axis by  $\gamma$ T3.

To assess whether  $\gamma$ T3 could preserve insulin sensitivity of adipocytes from the deleterious effects of IL-1 $\beta$ , primary mouse adipocytes differentiated from mesenchymal stem cells were first cultured with or without  $\gamma$ T3 (1  $\mu$ M). Then adipocyte cultures were exposed to the IL-1 $\beta$ -containing CM obtained from LPS/Ng-treated iJ774 (Fig. 5H, left). The insulin-stimulated Akt phosphorylation was significantly reduced following exposure to the CM (Fig. 5H,

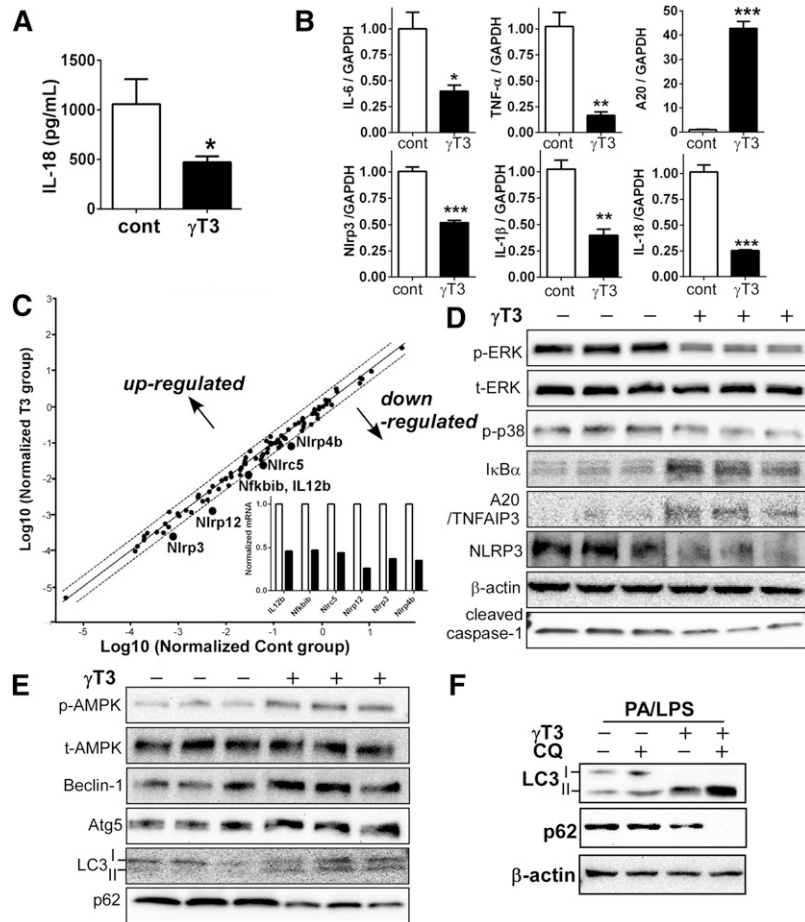


**Fig. 4.** Feeding  $\gamma$ T3 to *db/db* mice repressed the formation of NLRP3 inflammasomes in peritoneal macrophages. A: IL-18 levels (ELISA) in blood plasma collected from control and  $\gamma$ T3-fed *db/db* mice ( $n = 6$ ). B: The mRNA expression of *Il-6*, *Tnf $\alpha$* , *Il-1 $\beta$* , *Il-18*, *A20*, and *Nlrp3* analyzed by qPCR in isolated peritoneal macrophages ( $n = 6$ ). C: Microarray analysis of mouse inflammasome (84 genes) by qPCR. Pooled mRNA ( $n = 4$  per group) was used for analysis. Target genes positioned outside the space defined by the broken lines are differentially expressed by at least 2-fold. Insert: Fold change of downregulated genes (open bar, control macrophages; closed bar,  $\gamma$ T3-fed macrophages). D: Western blot analysis of p-ERK, t-ERK, p-p38, I $\kappa$ B $\alpha$ , A20, NLRP3, and cleaved caspase-1. E: Western blot analysis for p-AMPK and t-AMPK, and autophagy-related protein expression of Beclin-1, Atg5, LC3, and p62 (see supplementary Fig. 1 for quantification). F: BMDMs were stimulated for inflammasome formation by PA/LPS for 12 h. CQ (10  $\mu$ M, an autophagy inhibitor) was added 3 h before harvest. Protein levels of LC3I/II, p62, and  $\beta$ -actin were determined by Western blot ( $n = 3$ ). Data in A and B are expressed as mean  $\pm$  SEM. \*  $P < 0.05$ ; \*\*  $P < 0.01$ ; \*\*\*  $P < 0.001$ .

lane 5), unless the adipocytes had received  $\gamma$ T3 (Fig. 5H, lane 6). Collectively, these data demonstrate that  $\gamma$ T3 reduced NF $\kappa$ B and NLRP3 inflammasome activation in WAT resulting in attenuation of adipose tissue inflammation and preservation of insulin sensitivity.

#### $\gamma$ T3 blocked NF $\kappa$ B-mediated priming of the inflammasome

NF $\kappa$ B activation is a critical step for the priming of the inflammasomes. Based on multiple observations that  $\gamma$ T3 increased A20 expression (Figs. 4, 5), we hypothesized that  $\gamma$ T3 inhibits NF $\kappa$ B signaling pathway via activation of A20, an ubiquitination-editing enzyme. We further hypothesized that A20 activation hinders the ubiquitination of TRAF6. The formation of a polyubiquitin chain (K63-Ub) on TRAF6 is critical for TRAF6-mediated phosphorylation and activation of IKK. Following activation, IKK

phosphorylates I $\kappa$ B, which undergoes proteosomal degradation thereby allowing NF $\kappa$ B to dimerize into its active form (21). To test these hypotheses, BMDMs were pre-treated with or without  $\gamma$ T3 (1  $\mu$ M) and then stimulated with LPS, and mRNAs and proteins were collected over a 3 h time course. We found that *Il-1 $\beta$*  mRNA levels were inversely associated with those of *A20* (Fig. 6A). The elevation of A20 protein abundance induced by  $\gamma$ T3 coincided with: 1) the decrease of p-I $\kappa$ B kinase (IKK)  $\alpha/\beta$ , p-ERK, and p-I $\kappa$ B $\alpha$ ; 2) the reappearance of I $\kappa$ B $\alpha$ ; and 3) the disappearance of TRAF6, suggesting a negative feedback of A20 on TRAF6/IKK/NF $\kappa$ B signaling (Fig. 6B).

It has been shown that A20 can transfer TRAF6-bound Ub from residue K63 to K48 thereby causing the proteosomal degradation of TRAF6 (22). Thus, we performed immunoprecipitation to determine K63- versus K48-Ub status of TRAF6. As opposed to the study by Muroi and



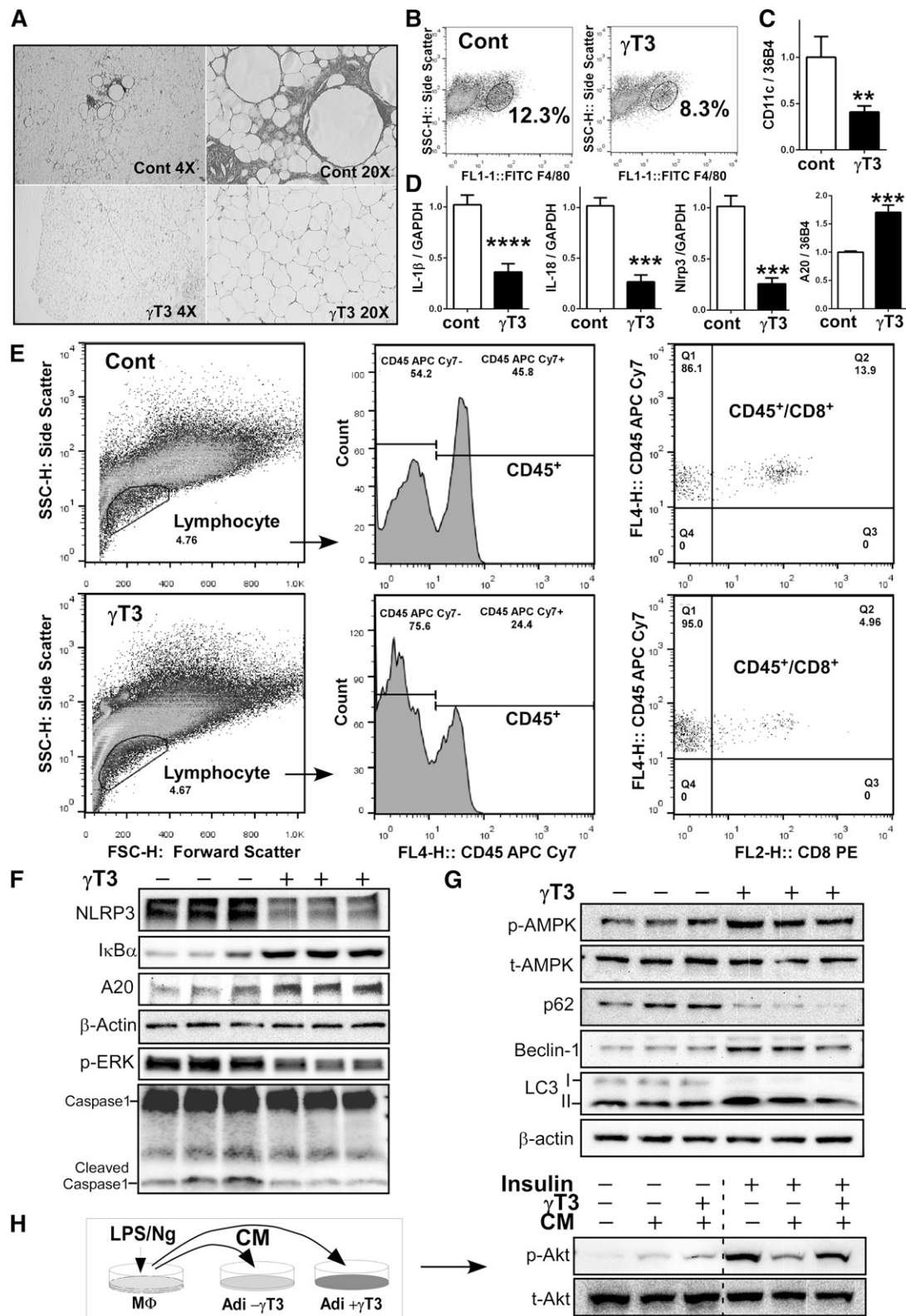


**Fig. 5.**  $\gamma$ T3 supplementation regulated innate immune system and insulin sensitivity in WAT. Epididymal adipose tissues were isolated from the control and  $\gamma$ T3-fed *db/db* mice. **A:** H and E staining. **B:** Flow cytometric determination of F4/80<sup>+</sup> population from adipose SV fraction (representative flow cytogram of four mice per group). **C:** *Cd11c* gene expression (n = 6). **D:** mRNA expression *Il-1 $\beta$* , *Il-18*, *Nlrp3*, and *A20* (n = 6). Data are expressed as mean  $\pm$  SEM. \*  $P < 0.05$ ; \*\*  $P < 0.01$ ; \*\*\*  $P < 0.001$ . **E:** CD45<sup>+</sup> and CD45<sup>+</sup>CD8<sup>+</sup> T-cell fractions by flow cytometry (representative flow cytogram of four mice per group). **F:** Western blot analysis of NLRP3, I $\kappa$ B $\alpha$ , A20/TNFAIP3, cleaved caspase-1, and  $\beta$ -actin (loading control). **G:** Western blot analysis of p-AMPK, t-AMPK, p62, Beclin-1, LC3, and  $\beta$ -actin. Each lane represents epididymal WAT from different animals (see supplementary Fig. 2 for quantification). **H:** Inflammasome formation was stimulated by LPS/Ng in iJ774 cells. Primary murine adipocytes were preincubated with  $\gamma$ T3 before receiving the CM of LPS/Ng-treated iJ774 (left). Insulin (100 nM)-stimulated levels of p-Akt and t-Akt were determined by Western blot analysis (right).

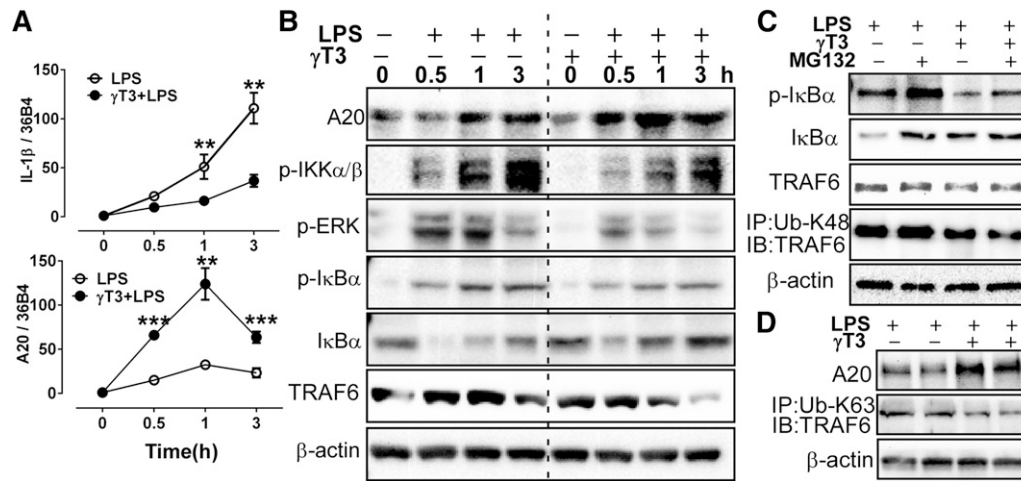


**Fig. 6.**  $\gamma$ T3 blocked NF $\kappa$ B-mediated priming of the inflammasome in BMDMs. BMDMs were pretreated with vehicle (–) or  $\gamma$ T3 (+) for 24 h. A, B: Cells were stimulated with LPS (100 ng/ml) at  $t = 0$  h, then total RNA and cellular proteins were extracted at 0, 0.5, 1, and 3 h. A: Temporal changes in mRNA levels of *IL-1 $\beta$*  and *A20* by qPCR. B: Temporal changes in protein abundance of A20, p-IKK, p-ERK, p-I $\kappa$ B $\alpha$ , I $\kappa$ B $\alpha$ , TRAF6, and  $\beta$ -actin by Western blot analysis. C: BMDMs were pretreated with proteasomal degradation inhibitor MG132 (50  $\mu$ M) prior to LPS stimulation (1 h). Protein levels of p-I $\kappa$ B $\alpha$ , I $\kappa$ B $\alpha$ , TRAF6, and  $\beta$ -actin were determined by Western blot. Cell extracts were immunoprecipitated (IP) with K48 ubiquitination antibody (Ub-K48) then immunoblotted (IB) with antibodies against TRAF6. D: BMDMs were stimulated with LPS for 1 h. Cell extracts were immunoprecipitated (IP) with K63 ubiquitination antibody (Ub-K63) then immunoblotted (IB) with antibodies against TRAF6. Data are shown as mean  $\pm$  SEM. \*\*  $P < 0.01$ ; \*\*\*  $P < 0.001$ .

Tanamoto (22), inhibition of proteasomal degradation by MG132 failed to rescue the  $\gamma$ T3-mediated decrease of TRAF6 or to increase K48-Ub of TRAF6 (Fig. 6C). Similarly,  $\gamma$ T3 also lowered K63-Ub of TRAF6 compared with controls (Fig. 6D). Taken together, we posit that A20 induction by  $\gamma$ T3 inhibited the ubiquitination of both the K48 and K63 residues of TRAF6 and promoted TRAF6 nonproteasomal degradation, leading to early blockage of the NF $\kappa$ B signaling pathway and repression of inflammasome priming.

#### Inhibition of A20 and AMPK activation altered IL-1 $\beta$ secretion and caspase-1 cleavage by $\gamma$ T3

To determine whether AMPK mediates  $\gamma$ T3's inhibition of the inflammasome, we treated iJ774 macrophages with Compound C (10  $\mu$ M), a chemical inhibitor of AMPK. Results showed that Compound C partially reversed  $\gamma$ T3-dependent decreases in IL-1 $\beta$  secretion (Fig. 7A), caspase-1 cleavage (Fig. 7B, top), and iGLuc activity (Fig. 7B, bottom). To ascertain the contribution of A20 induction by  $\gamma$ T3 in the lowering of IL-1 $\beta$  secretion and caspase-1 activation, A20 was knocked down in iJ774 macrophages using siRNAs. As expected, the silencing of A20 effectively decreased  $\gamma$ T3-mediated A20 induction but did not reverse  $\gamma$ T3-mediated blockage of caspase-1 cleavage (Fig. 7C). Although total IL-1 $\beta$  levels were significantly increased in siA20-transfected cells versus siControl cells, the extent to which  $\gamma$ T3 attenuated IL-1 $\beta$  secretion was not significantly different between siA20 and siControl cells ( $\Delta$  of columns 1 and 2 vs.  $\Delta$  of columns 3 and 4; Fig. 7D). Taken together, our results suggest that 1) AMPK mediates the blockage of caspase-1 cleavage afforded by  $\gamma$ T3, 2) A20 downregulates NF $\kappa$ B-mediated

production of IL-1 $\beta$ , and 3)  $\gamma$ T3 can inhibit IL-1 $\beta$  production independently of A20.

#### DISCUSSION

The activation of the NLRP3 inflammasome is positively associated with the prevalence of type 2 diabetes. Consequently, targeting the inhibition of NLRP3 inflammasome is an attractive strategy against type 2 diabetes. In this study, we addressed the question of whether  $\gamma$ T3, an unsaturated form of vitamin E, is effective in suppressing the NLRP3 inflammasome and mitigating the pathophysiological consequences of inflammation in a mouse model of type 2 diabetes. Our results showed that  $\gamma$ T3 inhibits the NLRP3 inflammasome activity by two-pronged mechanism: 1) the blockage of inflammasome priming and 2) the impediment of inflammasome activation. To our knowledge, this is the first study to characterize the role of  $\gamma$ T3 in inhibiting the NLRP3 inflammasome and show that, by acting through the inflammasome,  $\gamma$ T3 dietary supplementation can improve insulin resistance in mice.

Intense research is currently being devoted to the discovery of chemical inhibitors of the NLRP3 inflammasome (23), blocking agents of the IL-1 $\beta$  signaling such as IL-1R (IL-1 receptor) antagonist (24), and neutralizing antibodies (25, 26). Although, there is growing evidence that nutrition is a critical modulator of the inflammasome, few attempts have been made to inhibit the NLRP3 inflammasome through diet. For instance, elevated levels of circulating FFAs were shown to activate the NLRP3 inflammasome and weaken insulin sensitivity (27, 28). In contrast,  $\omega$ -3 FA (29) and MUFAs (30) have been shown to curtail NLRP3



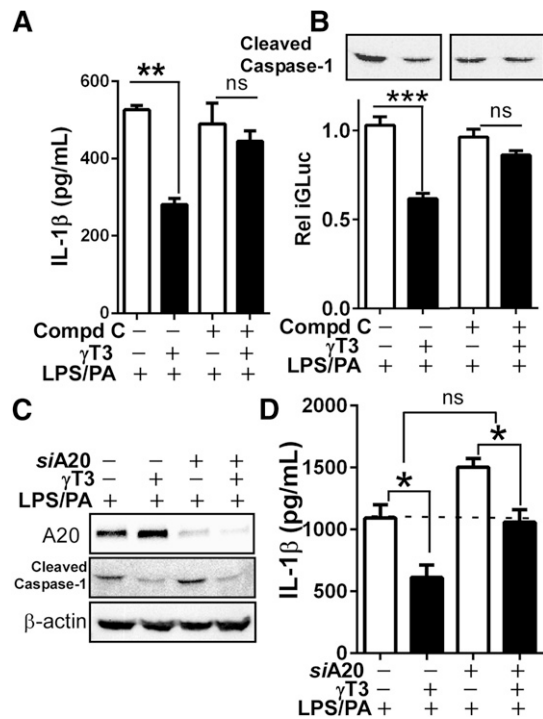


**Fig. 7.** AMPK and A20 contributed to  $\gamma$ T3-mediated lowering of IL-1 $\beta$  secretion. iJ774 macrophages were treated with Compound C (10  $\mu$ M) to inhibit AMPK (A–C) or transfected with either A20-targeting siRNA (siA20+) or nontargeting siRNA (siA20–) followed by LPS/PA stimulation for 12 h (C, D). A: Secreted IL-1 $\beta$  was measured by ELISA (n = 6). B: Relative GLuc activity of iGLuc (bottom) and caspase-1 cleavage (top). C: Western blot analysis of A20, cleaved caspase-1, and  $\beta$ -actin (representative of triplicate samples). D: Secreted IL-1 $\beta$  was measured by ELISA (n = 6). The dotted line indicates the basal IL-1 $\beta$  level of siCont cells primed with LPS/PA. All data are expressed as mean  $\pm$  SEM. \*  $P < 0.05$ ; \*\*  $P < 0.01$ ; \*\*\*  $P < 0.001$ . ns, nonsignificant.

inflammasome activation. In this study, we report on the previously unrecognized function of  $\gamma$ T3 [at physiologically relevant concentration (1)] as a potent negative regulator of the NLRP3 inflammasome. Our data clearly show that  $\gamma$ T3 inhibited the NLRP3 inflammasome in three macrophage models [i.e., iJ774 macrocytic cells (Fig. 1), primary BMDMs (Fig. 2), and peritoneal macrophages freshly isolated from *db/db* mice (Fig. 4)]. In addition, the suppression of NLRP3 inflammasomes by  $\gamma$ T3 was evident upon stimulation of PAMP with Ng, and of DAMP with PA (Fig. 2). We also found that  $\gamma$ T3 altered the NLR-subset inflammasome, but not the AIM2-scaffold inflammasome, the adaptor protein ASC, or the other caspases (Fig. 4C), suggesting that  $\gamma$ T3 has therapeutic potential against metabolic diseases where the NLRP3 inflammasome is implicated, such as obesity, atherosclerosis, and type 2 diabetes (8).

In the obese, the chronic stimulation of Toll-like receptor 4 by FAs has been shown to activate the NLRP3 inflammasome of macrophages residing in the adipose tissue and provoke the massive influx of immune cells into WAT (27, 31). Here, we investigated the potential mitigating properties of dietary  $\gamma$ T3 on the inflammatory and immunological consequences of obesity toward glycemia, insulinemia, and WAT remodeling. To that end, we determined

the composition of NLRP3 inflammasomes, the extent of immune cell infiltration, and insulin sensitivity. We found that the lowering of NLRP3 inflammasome in the WAT of  $\gamma$ T3-fed mice (Fig. 5F) was associated with the lowering of cytotoxic CD8<sup>+</sup> T cells and macrophages in WAT (Fig. 5A, B), and with the amelioration of insulin resistance (Figs. 3, 5H).


The destruction of pancreatic  $\beta$ -cells and impairment of insulin production are hallmarks of late-stage type 2 diabetes (32, 33). Because of a lack of specimens, we were unable to determine whether the protection of  $\beta$  cells afforded by  $\gamma$ T3 (Fig. 3I–L) was due to the blockage of inflammasome formation within the islets or the insensitivity of  $\beta$  cells to the deleterious effects of IL-1 $\beta$  paracrine signaling. We are currently investigating whether  $\gamma$ T3 inhibits the inflammasome of macrophages residing in islets or the inflammasome of  $\beta$  cells themselves, or both.

Mechanistically, we had anticipated that  $\gamma$ T3 would inhibit the priming of NLRP3 inflammasome based on  $\gamma$ T3's intrinsic ability to suppress NF $\kappa$ B (5). However, we did not anticipate that  $\gamma$ T3 would augment A20 induction, an ubiquitin-editing enzyme (34). Single nucleotide polymorphisms in the *Tnfrsf25/A20* are associated with increased susceptibility to chronic inflammatory diseases (35, 36). Deletion of A20 has been shown to cause hypersensitivity to TNF- $\alpha$  due to the constitutive activation of NF $\kappa$ B, leading to premature death (37). In addition, an inverse correlation between diabetes incidence and A20 mRNA levels was found in patients with both type 1 and type 2 diabetes (38). In our study, multiple lines of evidence demonstrated that A20 is augmented by  $\gamma$ T3 to mitigate the priming of the NLRP3 inflammasome (Figs. 4, 6, and 7). Recently, Wang et al. (39) have reported that  $\gamma$ T3 causes A20 induction via regulation of sphingolipid metabolism. It is presently unknown whether alterations to sphingolipid metabolism by  $\gamma$ T3 affected NLRP3 inflammasome activity in our study. Nonetheless, the work by Wang et al. corroborates our claim that  $\gamma$ T3 protects against abnormal stimulation of the innate immune system in part through the upregulation of A20 and feedback inhibition of priming of the NLRP3 inflammasome. Indeed, A20 silencing with siRNA did not completely reverse  $\gamma$ T3's inhibition of IL-1 $\beta$  secretion (Fig. 7C, D), suggesting that A20 activation is important but not sufficient, and full inhibition of NLRP3 inflammasome necessitates the coordinated involvement of additional factors. One of these factors may be autophagy because Matsuzawa et al. (40) reported that A20 activation and autophagy cooperate in T-cell survival.

Autophagy regulates the fate of inflammasomes by engulfing PAMP and DAMP signals (41, 42). We clearly demonstrated that  $\gamma$ T3 activates AMPK and autophagy (Figs. 2, 4, and 5). We further showed that the inhibition of AMPK with Compound C almost completely reversed  $\gamma$ T3's suppression of NLRP3 inflammasome and caspase-1 cleavage, indicating that AMPK activation is critically important in the mechanism of  $\gamma$ T3 (Fig. 7). Further research exploring the cross-talks between the A20 and AMPK/autophagy signaling pathways is needed to fully understand the

precise mechanism by which  $\gamma$ T3 suppresses NLRP3 inflammasome activation.

Most tocotrienol dietary supplements are provided as mixed formulations of  $\alpha$ -,  $\gamma$ -, and  $\delta$ -tocotrienols, with the exception of tocotrienol supplementation isolated from annatto seeds, which contain >90% of  $\delta$ -tocotrienol. The bioavailability of  $\gamma$ T3 has been shown to vary in humans depending on the tocotrienol composition of the dietary source, the target population, and the study design (reviewed in Ref. 43). Tocotrienols circulate in blood bound to lipoproteins, in particular to HDL particles, suggesting that the plasma lipoprotein profile affects tocotrienol metabolism. Due to the low binding affinity of tocotrienols for the  $\alpha$ -tocopherol transfer protein, the transfer of tocotrienols to HDL particles must occur via alternative, yet to be identified pathways (44, 45). The tocotrienol-rich fraction supplementations are considered safe. They obtained the GRAS (Generally Recognized as Safe) designation from the Food and Drug Administration. Based on a recent review by Podszun et al. (46), there is no clear evidence that high doses of vitamin E (>300 mg/day), either as tocotrienols or tocopherols, cause adverse effects in either animals or humans. However, we note that a meta-analysis of human studies with vitamin E raised some concerns with regard to high-dose vitamin E supplementation, which may have adverse effects when consumed with certain drugs, such as aspirin (47). Despite some uncertainties regarding the metabolism of tocotrienols, multiple clinical studies support their beneficial effects against metabolic diseases (48). By showing that  $\gamma$ T3 inhibits the NLRP3 inflammasome and considering that the innate immune response plays a central role in metabolic disorders, our study may provide a possible explanation for some of the clinical positive outcomes of tocotrienol supplementation (8).

In summary, the critical role of the NLRP3 inflammasome in the pathophysiology of insulin resistance was confirmed in human studies (49, 50). Hence, by revealing that  $\gamma$ T3 supplementation blunts NLRP3 inflammasome activity and delays the progression of type 2 diabetes, our present work has clinical relevance. Although further investigations in human subjects are necessary to validate the therapeutic applicability of our work, we herein present seminal evidence that  $\gamma$ T3 is an anti-inflammatory vitamin by inhibiting the NLRP3 inflammasome in macrophages. 

The authors thank Dr. Hornung at the University of Bonn for providing the iGLuc reporter for inflammasome assay.

## REFERENCES

- Jiang, Q. 2014. Natural forms of vitamin E: metabolism, antioxidant, and anti-inflammatory activities and their role in disease prevention and therapy. *Free Radic. Biol. Med.* **72**: 76–90.
- Burdeos, G. C., K. Nakagawa, F. Kimura, and T. Miyazawa. 2012. Tocotrienol attenuates triglyceride accumulation in HepG2 cells and F344 rats. *Lipids*. **47**: 471–481.
- Siddiqui, S., H. Ahsan, M. R. Khan, and W. A. Siddiqui. 2013. Protective effects of tocotrienols against lipid-induced nephropathy in experimental type-2 diabetic rats by modulation in TGF-beta expression. *Toxicol. Appl. Pharmacol.* **273**: 314–324.
- Haghighat, N., M. Vafa, S. Eghtesadi, I. Heidari, A. Hosseini, and A. Rostami. 2014. The effects of tocotrienols added to canola oil on microalbuminuria, inflammation, and nitrosative stress in patients with type 2 diabetes: a randomized, double-blind, placebo-controlled trial. *Int. J. Prev. Med.* **5**: 617–623.
- Zhao, L., I. Kang, X. Fang, W. Wang, M. A. Lee, R. R. Hollins, M. R. Marshall, and S. Chung. 2015. Gamma-tocotrienol attenuates high-fat diet-induced obesity and insulin resistance by inhibiting adipose inflammation and M1 macrophage recruitment. *Int. J. Obes. (Lond.)*. **39**: 438–446.
- Ahn, K. S., G. Sethi, K. Krishnan, and B. B. Aggarwal. 2007. Gamma-tocotrienol inhibits nuclear factor-kappaB signaling pathway through inhibition of receptor-interacting protein and TAK1 leading to suppression of antiapoptotic gene products and potentiation of apoptosis. *J. Biol. Chem.* **282**: 809–820.
- Wang, Y., and Q. Jiang. 2013. gamma-Tocotrienol inhibits lipopolysaccharide-induced interleukin-6 and granulocyte colony-stimulating factor by suppressing C/EBPbeta and NF-kappaB in macrophages. *J. Nutr. Biochem.* **24**: 1146–1152.
- Ozaki, E., M. Campbell, and S. L. Doyle. 2015. Targeting the NLRP3 inflammasome in chronic inflammatory diseases: current perspectives. *J. Inflamm. Res.* **8**: 15–27.
- Stienstra, R., C. J. Tack, T. D. Kanneganti, L. A. Joosten, and M. G. Netea. 2012. The inflammasome puts obesity in the danger zone. *Cell Metab.* **15**: 10–18.
- Stienstra, R., J. A. van Diepen, C. J. Tack, M. H. Zaki, F. L. van de Veerdonk, D. Perera, G. A. Neale, G. J. Hooiveld, A. Hijmans, I. Vroegrijk, et al. 2011. Inflammasome is a central player in the induction of obesity and insulin resistance. *Proc. Natl. Acad. Sci. USA*. **108**: 15324–15329.
- Vandanmagsar, B., Y. H. Youm, A. Ravussin, J. E. Galgani, K. Stadler, R. L. Mynatt, E. Ravussin, J. M. Stephens, and V. D. Dixit. 2011. The NLRP3 inflammasome instigates obesity-induced inflammation and insulin resistance. *Nat. Med.* **17**: 179–188.
- Latz, E., T. S. Xiao, and A. Stutz. 2013. Activation and regulation of the inflammasomes. *Nat. Rev. Immunol.* **13**: 397–411.
- Bauernfeind, F. G., G. Horvath, A. Stutz, E. S. Alnemri, K. MacDonald, D. Speert, T. Fernandes-Alnemri, J. Wu, B. G. Monks, K. A. Fitzgerald, et al. 2009. Cutting edge: NF-kappaB activating pattern recognition and cytokine receptors license NLRP3 inflammasome activation by regulating NLRP3 expression. *J. Immunol.* **183**: 787–791.
- Martins, J. D., J. Liberal, A. Silva, I. Ferreira, B. M. Neves, and M. T. Cruz. 2015. Autophagy and inflammasome interplay. *DNA Cell Biol.* **34**: 274–281.
- Rickmann, M., E. C. Vaquero, J. R. Malagelada, and X. Molero. 2007. Tocotrienols induce apoptosis and autophagy in rat pancreatic stellate cells through the mitochondrial death pathway. *Gastroenterology*. **132**: 2518–2532.
- Tiwari, R. V., P. Parajuli, and P. W. Sylvester. 2015. gamma-Tocotrienol-induced endoplasmic reticulum stress and autophagy act concurrently to promote breast cancer cell death. *Biochem. Cell Biol.* **93**: 306–320.
- Wu, S. J., G. Y. Huang, and L. T. Ng. 2013. gamma-Tocotrienol induced cell cycle arrest and apoptosis via activating the Bax-mediated mitochondrial and AMPK signaling pathways in 3T3-L1 adipocytes. *Food Chem. Toxicol.* **59**: 501–513.
- Zhao, L., J. H. Ha, M. Okla, and S. Chung. 2014. Activation of autophagy and AMPK by gamma-tocotrienol suppresses the adipogenesis in human adipose derived stem cells. *Mol. Nutr. Food Res.* **58**: 569–579.
- Bartok, E., F. Bauernfeind, M. G. Khaminets, C. Jakobs, B. Monks, K. A. Fitzgerald, E. Latz, and V. Hornung. 2013. iGLuc: a luciferase-based inflammasome and protease activity reporter. *Nat. Methods*. **10**: 147–154.
- Orr, J. S., A. J. Kennedy, and A. H. Hasty. 2013. Isolation of adipose tissue immune cells. *J. Vis. Exp.* **75**: 50707.
- Boone, D. L., E. E. Turer, E. G. Lee, R. C. Ahmad, M. T. Wheeler, C. Tsui, P. Hurley, M. Chien, S. Chai, O. Hitotsumatsu, et al. 2004. The ubiquitin-modifying enzyme A20 is required for termination of Toll-like receptor responses. *Nat. Immunol.* **5**: 1052–1060.
- Muroi, M., and K. Tanamoto. 2012. IRAK-1-mediated negative regulation of Toll-like receptor signaling through proteasome-dependent downregulation of TRAF6. *Biochim. Biophys. Acta*. **1823**: 255–263.
- Coll, R. C., A. A. Robertson, J. J. Chae, S. C. Higgins, R. Munoz-Planillo, M. C. Inserra, I. Vetter, L. S. Dungan, B. G. Monks, A.

- Stutz, et al. 2015. A small-molecule inhibitor of the NLRP3 inflammasome for the treatment of inflammatory diseases. *Nat. Med.* **21**: 248–255.
24. Larsen, C. M., M. Faulenbach, A. Vaag, A. Volund, J. A. Ehres, B. Seifert, T. Mandrup-Poulsen, and M. Y. Donath. 2007. Interleukin-1-receptor antagonist in type 2 diabetes mellitus. *N. Engl. J. Med.* **356**: 1517–1526.
  25. Dinarello, C. A., and J. W. van der Meer. 2013. Treating inflammation by blocking interleukin-1 in humans. *Semin. Immunol.* **25**: 469–484.
  26. Jesus, A. A., and R. Goldbach-Mansky. 2014. IL-1 blockade in auto-inflammatory syndromes. *Annu. Rev. Med.* **65**: 223–244.
  27. Wen, H., D. Gris, Y. Lei, S. Jha, L. Zhang, M. T. Huang, W. J. Brickey, and J. P. Ting. 2011. Fatty acid-induced NLRP3-ASC inflammasome activation interferes with insulin signaling. *Nat. Immunol.* **12**: 408–415.
  28. Reynolds, C. M., F. C. McGillicuddy, K. A. Harford, O. M. Finucane, K. H. Mills, and H. M. Roche. 2012. Dietary saturated fatty acids prime the NLRP3 inflammasome via TLR4 in dendritic cells—implications for diet-induced insulin resistance. *Mol. Nutr. Food Res.* **56**: 1212–1222.
  29. Yan, Y., W. Jiang, T. Spinetti, A. Tardivel, R. Castillo, C. Bourquin, G. Guarda, Z. Tian, J. Tschopp, and R. Zhou. 2013. Omega-3 fatty acids prevent inflammation and metabolic disorder through inhibition of NLRP3 inflammasome activation. *Immunity.* **38**: 1154–1163.
  30. Finucane, O. M., C. L. Lyons, A. M. Murphy, C. M. Reynolds, R. Klinger, N. P. Healy, A. A. Cooke, R. C. Coll, L. McAllan, K. N. Nilaweera, et al. 2015. Monounsaturated fatty acid-enriched high-fat diets impede adipose NLRP3 inflammasome-mediated IL-1 $\beta$  secretion and insulin resistance despite obesity. *Diabetes.* **64**: 2116–2128.
  31. Nishimura, S., I. Manabe, M. Nagasaki, K. Eto, H. Yamashita, M. Ohsugi, M. Otsu, K. Hara, K. Ueki, S. Sugiura, et al. 2009. CD8<sup>+</sup> effector T cells contribute to macrophage recruitment and adipose tissue inflammation in obesity. *Nat. Med.* **15**: 914–920.
  32. Potter, K. J., C. Y. Westwell-Roper, A. M. Klimek-Abercrombie, G. L. Warnock, and C. B. Verchere. 2014. Death and dysfunction of transplanted beta-cells: lessons learned from type 2 diabetes? *Diabetes.* **63**: 12–19.
  33. Weir, G. C., and S. Bonner-Weir. 2004. Five stages of evolving beta-cell dysfunction during progression to diabetes. *Diabetes.* **53** (Suppl. 3): S16–S21.
  34. Vereecke, L., R. Beyaert, and G. van Loo. 2009. The ubiquitin-editing enzyme A20 (TNFAIP3) is a central regulator of immunopathology. *Trends Immunol.* **30**: 383–391.
  35. Mele, A., J. R. Cervantes, V. Chien, D. Friedman, and C. Ferran. 2014. Single nucleotide polymorphisms at the TNFAIP3/A20 locus and susceptibility/resistance to inflammatory and autoimmune diseases. *Adv. Exp. Med. Biol.* **809**: 163–183.
  36. Vereecke, L., R. Beyaert, and G. van Loo. 2011. Genetic relationships between A20/TNFAIP3, chronic inflammation and autoimmune disease. *Biochem. Soc. Trans.* **39**: 1086–1091.
  37. Lee, E. G., D. L. Boone, S. Chai, S. L. Libby, M. Chien, J. P. Lodolce, and A. Ma. 2000. Failure to regulate TNF-induced NF- $\kappa$ B and cell death responses in A20-deficient mice. *Science.* **289**: 2350–2354.
  38. Cheng, L., D. Zhang, Y. Jiang, W. Deng, Q. Wu, X. Jiang, and B. Chen. 2014. Decreased A20 mRNA and protein expression in peripheral blood mononuclear cells in patients with type 2 diabetes and latent autoimmune diabetes in adults. *Diabetes Res. Clin. Pract.* **106**: 611–616.
  39. Wang, Y., N. Y. Park, Y. Jang, A. Ma, and Q. Jiang. 2015. Vitamin E gamma-tocotrienol inhibits cytokine-stimulated NF- $\kappa$ B activation by induction of anti-inflammatory A20 via stress adaptive response due to modulation of sphingolipids. *J. Immunol.* **195**: 126–133.
  40. Matsuzawa, Y., S. Oshima, M. Takahara, C. Maeyashiki, Y. Nemoto, M. Kobayashi, Y. Nibe, K. Nozaki, T. Nagaishi, R. Okamoto, et al. 2015. TNFAIP3 promotes survival of CD4 T cells by restricting mTOR and promoting autophagy. *Autophagy.* **11**: 1052–1062.
  41. Wang, Y., Y. B. Li, J. J. Yin, Y. Wang, L. B. Zhu, G. Y. Xie, and S. H. Pan. 2013. Autophagy regulates inflammation following oxidative injury in diabetes. *Autophagy.* **9**: 272–277.
  42. Yuk, J. M., and E. K. Jo. 2013. Crosstalk between autophagy and inflammasomes. *Mol. Cells.* **36**: 393–399.
  43. Fu, J. Y., H. L. Che, D. M. Tan, and K. T. Teng. 2014. Bioavailability of tocotrienols: evidence in human studies. *Nutr. Metab. (Lond).* **11**: 5.
  44. Khosla, P., V. Patel, J. M. Whinter, S. Khanna, M. Rakhkovskaya, S. Roy, and C. K. Sen. 2006. Postprandial levels of the natural vitamin E tocotrienol in human circulation. *Antioxid. Redox Signal.* **8**: 1059–1068.
  45. Fairus, S., R. M. Nor, H. M. Cheng, and K. Sundram. 2006. Postprandial metabolic fate of tocotrienol-rich vitamin E differs significantly from that of  $\alpha$ -tocopherol. *Am. J. Clin. Nutr.* **84**: 835–842.
  46. Podszun, M., and J. Frank. 2014. Vitamin E-drug interactions: molecular basis and clinical relevance. *Nutr. Res. Rev.* **27**: 215–231.
  47. Bjelakovic, G., D. Nikolova, L. L. Gluud, R. G. Simonetti, and C. Gluud. 2007. Mortality in randomized trials of antioxidant supplements for primary and secondary prevention: systematic review and meta-analysis. *J. Am. Med. Assoc.* **297**: 842–857.
  48. Aggarwal, B. B., C. Sundaram, S. Prasad, and R. Kannappan. 2010. Tocotrienols, the vitamin E of the 21st century: its potential against cancer and other chronic diseases. *Biochem. Pharmacol.* **80**: 1613–1631.
  49. Esser, N., L. L'homme, R. A. De, L. Kohnen, A. J. Scheen, M. Moutschen, J. Piette, S. Legrand-Poels, and N. Paquot. 2013. Obesity phenotype is related to NLRP3 inflammasome activity and immunological profile of visceral adipose tissue. *Diabetologia.* **56**: 2487–2497.
  50. Lee, H. M., J. J. Kim, H. J. Kim, M. Shong, B. J. Ku, and E. K. Jo. 2013. Upregulated NLRP3 inflammasome activation in patients with type 2 diabetes. *Diabetes.* **62**: 194–204.